

RSC Advances



This is an *Accepted Manuscript*, which has been through the Royal Society of Chemistry peer review process and has been accepted for publication.

Accepted Manuscripts are published online shortly after acceptance, before technical editing, formatting and proof reading. Using this free service, authors can make their results available to the community, in citable form, before we publish the edited article. This *Accepted Manuscript* will be replaced by the edited, formatted and paginated article as soon as this is available.

You can find more information about *Accepted Manuscripts* in the [Information for Authors](#).

Please note that technical editing may introduce minor changes to the text and/or graphics, which may alter content. The journal's standard [Terms & Conditions](#) and the [Ethical guidelines](#) still apply. In no event shall the Royal Society of Chemistry be held responsible for any errors or omissions in this *Accepted Manuscript* or any consequences arising from the use of any information it contains.

Cite this: DOI: 10.1039/c0xx00000x

www.rsc.org/xxxxxx

ARTICLE TYPE

Three-Dimensional NiAl-Mixed Metal Oxide Film: Preparation and Capacitive Deionization Performances

Xiaodong Lei,* Bo Wang, Junfeng Liu, Zhengping Ye, Zheng Chang, Meihong Jiang and Xiaoming Sun

Received (in XXX, XXX) Xth XXXXXXXXX 20XX, Accepted Xth XXXXXXXXX 20XX

DOI: 10.1039/b000000x

NiAl layered double hydroxide (NiAl-LDH) film was grown on the surface of three-dimensional (3D) nickel foam by an in situ hydrothermal method using nickel foam substrate as nickel source, and boehmite (AlOOH) sol as aluminium source. 3D NiAl-mixed metal oxide (NiAl-MMO) film was obtained by calcined NiAl-LDH film at 400 °C. The structure and surface morphology of film samples were studied by X-ray diffraction, elemental analysis, room temperature Fourier transform infrared spectra and electron microscopy analysis. These results showed that NiAl-LDH nanoplatelets densely covered on the surface of nickel foam substrate. The 3D NiAl-MMO film obtained by calcined NiAl-LDH film was used as capacitive deionization (CDI) electrode for electrosorption of NaCl in water. Under static test conditions, the electrosorption ratio for 0.01 mol L⁻¹ NaCl is above 37.5%, while the electrosorptive capacity of the electrode is ultrahigh about 81.2 mg g⁻¹ electrode. For 15 times electrosorption and desorption cycling, the decreasing of electrosorption ratio is very little, and the desorption ratio of NaCl is above 87.7%. It is indicated that the NiAl-MMO film electrode can be used for the removal of NaCl in water.

Introduction

Concern about environmental protection has increased over the years from a global viewpoint. Throughout the past several decades, an increasing trend in the extensive emission of various organic and inorganic pollutants into the ecosystems has been witnessed.¹ It is important to recycle and reuse some of the wastewater and turn salt water into fresh water.² Traditional NaCl removal technologies involve ion exchange, distillation, electrodialysis, reverse osmosis and adsorption, etc. However, all these technologies have their own disadvantages. For example, ion exchange may cause secondary pollution,³ and distillation may cost high energy. The adoption of environmental electrochemical approach, electrosorption or CDI which combines the enhancement of adsorption rate and capacity by polarization and electrochemical regeneration *in situ*,⁴ has received extensive stern consideration.⁵ Compared with other adsorption technology, electrosorption is an economical and effective method with many advantages such as low cost, long life cycle, easy regeneration, energy conservation, and without secondary pollution.⁶ Similar to the traditional adsorption, the development of electric adsorbent is one of the key factors of adsorption. At present, the main electrosorption electrode materials include graphite, granular activated carbon (GAC), activated carbon (AC) sheets, AC fibre, carbon aerogels, carbon nanotube (CNT), and so on.⁷ However, these materials have shortcomings, such as little adsorption capacity of graphite, high resistance and mass transfer resistance of GAC, harsh preparation conditions of carbon aerogels, and high cost of CNT, which

limited their massive investment in industrial applications.⁷

Layered double hydroxides (LDHs), also known as hydrotalcite-like materials or anionic clays, are a class of lamellar compounds made up of positively charged layers with an interlayer region containing charge compensating anions and solvent molecules. They are generally expressed by the formula $[M_{1-x}^{2+}M_x^{3+}(\text{OH})_2]^{x+}(\text{A}^{n-})_{x/n}\cdot y\text{H}_2\text{O}$, where M²⁺ represents a divalent metal cation, M³⁺ a trivalent metal cation and Aⁿ⁻ an anion. *x* ranges from 0.15 to 0.33 for pure LDH formation, and *y* is typically of the order 1 – 2.⁸ LDHs have surface areas of 20 – 120 m² g⁻¹ and high ion-exchange capacities and can be used to adsorb a variety of anionic pollutants. Materials with increased specific surface areas can be obtained by calcination of these LDHs at moderate temperatures, which affords mixed metal oxides (MMOs) with a homogeneous dispersion of metal cations.⁹ Calcined LDHs (MMOs) are promising adsorbents and have been widely used for removal of contaminant anions from wastewater.¹⁰ However, the obtained MMOs can be reconstructed to LDHs by anions intercalating. Regenerating MMOs need another calcining process, and the calcination is easy to cause secondary pollution.¹¹ If external electrostatic field is imposed to the surface of MMOs, the large surface area MMO would adsorb anions, and external electrostatic field can prevent MMOs to be transformed to LDHs by the anions. However, MMOs are insulating, it is necessary to immobilize MMOs on conductive substrate before MMOs are used as electrodes for electrosorption, highlighting the importance of direct growth of nanomaterials on nickel foam to impart intimate interactions and efficient charge

transport between the active MMO materials and the conductive substrate. For the purpose of developing novel innovative applications of LDHs as materials for supercapacitors,¹² corrosion-resistant coatings,¹³ or components in optical and magnetic devices,¹⁴ intensive studies have been conducted aimed at organizing LDH microcrystals into large uniformly aligned 2D arrays or films. Several methods have been employed to fabricate LDH films on different conductive substrates. For example, LDH microcrystals have been deposited on platinum disks and gold electrode surfaces from colloidal suspensions in order to prepare LDH films for electrode modification by deposition and Langmuir–Blodgett methods.¹⁵ Wang *et al.* successfully obtained NiAl–LDH nanoplatelets on the surface of nickel foam by a simple *in situ* precipitation method.¹⁶ The physical coating of NiAl–LDH on nickel foam is difficult to be used as electrode because the MMO dropped from the substrate easily during calcination. Therefore, NiAl–LDH films grown on the surface of conductive substrates is important for using the related MMO films for electrosorption. Recently, our group has reported *in situ* growth of LDHs on different metals, such as aluminum, copper and nickel foam.¹⁷ Many metal oxides/hydroxides, such as Ni(OH)₂,¹⁸ Co(OH)₂,¹⁹ Co_xNi_{1-x}(OH)₂,²⁰ Co₃O₄,²¹ ZnCo₂O₄,²² CoO–Li₂O composite,²³ Ni–Cu double hydroxide,²⁴ Ni–Mn oxide²⁵ and lithiated MnO₂,²⁶ have been fabricated on nickel foam by chemical methods and can be used as pseudocapacitive electrodes, cathodes of semi-fuel cell, lithium ion batteries and catalysts, respectively. Based on these researches, we can obtain immobilized MMO films on conducting nickel foam and use them as fine noncarbon electrodes for electrosorption.

In this paper, we introduce the fabrication of NiAl–LDH film using a 3D substrate of nickel foam by an *in situ* hydrothermal reaction. 3D NiAl–MMO film was obtained by calcining the NiAl–LDH film. The electrosorption properties of the NiAl–MMO film was investigated in detail. Compared with the carbon electrodes reported in other literatures, NiAl–MMO film electrode has shorter adsorption equilibrium time, higher electrosorption and desorption ratios and ultrahigh capacity. Therefore, NiAl–MMO film derived from NiAl–LDH film is excellent noncarbon electrosorption electrode candidate and it would be promising in the CDI industry.

Experimental section

Materials

Nickel foam (99.5% purity) was bought from Hanbo environmental equipment Co. Ltd., China. Aluminum isopropoxide (99.5% purity) was purchased from Sinopharm Chemical Reagent Co. Ltd. Graphite electrodes were purchased from Henan Jiaozuo Oriental Graphite Co. Ltd. All other reagents are analytical grade that purchased from Beijing chemical reagent company.

Preparation of NiAl–LDH and NiAl–MMO Films

Nickel foams (20 mm × 30 mm × 1.0 mm, weight 0.216 g) were degreased with acetone, etched with 6.0 mol L⁻¹ HCl for 15 min, rinsed with water, and then dried in an oven at 60 °C. The treated nickel foams were used for NiAl–LDH film substrates.

The preparation of AlOOH sol: 6.476 g of aluminum isopropoxide was dissolved in 400 mL of 0.05 mol L⁻¹ nitric acid,

the solution was stirred for 10 min in air at room temperature, then heated to 90 °C in the water bath for about 6 h and AlOOH sol was formed.

With vigorous stirring, added NH₃·H₂O solution dropwise into 40 mL AlOOH sol until the pH reached 7.5 under room temperature. The resulting suspension with a piece of nickel foam was transferred to 50 mL Teflon-lined stainless-steel autoclave, which was sealed, maintained at 120 °C for 36 h. At last, the NiAl–LDH film on nickel foam was obtained by dried the sample at 60 °C for 10 h. The prepared NiAl–LDH film was calcined at 400 °C for 3 h. After cooling, NiAl–LDH film was transformed to NiAl–MMO film which can be used as electrode for electrosorption.

Electrosorption Tests

To measure the electrosorption and desorption of ions on electrodes, batch-mode experiments were conducted in a 100 mL beaker. A piece of graphite (20 mm × 30 mm × 1.0 mm) and a piece of NiAl–MMO film were used as electrodes that placed face to face at both sides of a spacer with 2 cm and connected with a DC power supply. The volume of 0.01 mol L⁻¹ NaCl solution was 60 mL. After electrosorption reached equilibrium, the amount of electrosorbed NaCl was measured by applying a direct voltage of 1.2 V between two electrodes until a new equilibrium reached. Regeneration was accomplished by applying a reverse voltage of -1.2 V for 40 min and then turning off the power supply. Chloride anion concentration was measured with a PXS-270 ion meter (Shanghai Leici Instrument Company) by using chloride ion selective electrode and 232 type reference electrode. The corresponding concentration could be obtained with a calibration curve made prior to the experiments.

Characterization

Scanning electron microscopy (SEM) microanalyses of the samples were made using a Hitachi S4700 apparatus with the applied voltage of 20 kV, combined with energy dispersive X-ray spectroscopy (EDS) for the determination of metal composition. High resolution transmission electron microscopy (HRTEM) was carried on a JEM-3010 high resolution transmission electron microscopy at an accelerating voltage of 200 kV. For HRTEM analysis, a droplet of the ultrasonically dispersed samples in ethanol was placed onto an amorphous carbon-coated copper grid and then dried at air. Powder X-ray diffraction (XRD) patterns were obtained in the 2θ range 3 – 70° using a Shimadzu XRD-6000 diffractometer with Cu Kα radiation (λ = 0.15406 nm, 40 kV and 30 mA) at a scanning rate of 5° min⁻¹. Room temperature Fourier transform infrared (FT-IR) spectra were recorded in the range 4000 – 400 cm⁻¹ with 2 cm⁻¹ resolution on a Bruker Vector 22 Fourier transform spectrometer using the KBr pellet technique (1 mg of sample in 100 mg of KBr). Elemental analyses for metal elements were performed with a Shimadzu ICPS-7500 model inductively coupled plasma emission spectrometer (ICP-ES) with all samples being dissolved in dilute HNO₃ (1:1). The NiAl–MMO films (1 cm²) were used as the working electrodes. A platinum electrode (1 cm²) and an Ag/AgCl electrode were used as the counter and reference electrodes respectively. And the prepared 0.01 mol L⁻¹ NaCl aqueous solution was used as the electrolyte. The electrochemical performances of the NiAl–MMO films were researched on a CHI660D (Chen Hua, Shang Hai)

workstation for cyclic voltammetry (CV) and galvanostatic discharge tests.

Results and Discussion

Structure of As-synthesized Films

The growth of NiAl-LDH films on 3D nickel foam substrate were based on the reaction of AIOOH sol in diluted ammonium solution and nickel foam which involves the transportation of metal ions to the nickel foam surface, adsorption and enrichment of the ions on the substrate, and nucleation and growth of NiAl-LDH crystals. Appropriate pH was required (usually close to neutral or alkaline) because when the pH was about 7.5, a part of nickel dissolved in the AIOOH sol under the reaction with ammonium ions. Nickel foam has a 3D network structure, which greatly increases the surface area of substrate. Fig. 1a and b display the morphology of the NiAl-LDH film grown on the nickel foam substrate. It can be seen that the LDH film has grown on the nickel foam vertically and uniformly, in general, each crystal with a hexagon shape. Obviously, the (001) planes of NiAl-LDH crystals were almost perpendicular to the surface of the substrate (Fig. 1b). Fig. 1c shows the cross section of NiAl-LDH film. It indicates that NiAl-LDH film grown on the substrate tightly, the thickness of NiAl-LDH layer was about 500 nm. Due to some of nickel dissolved in the ammonium solution, the mass of the NiAl-LDH film with substrate (ca. 0.186 g, 20 mm × 30 mm × 1.0 mm) was slightly lighter than that of the initial nickel foam (ca. 0.216 g), and the load of NiAl-LDH on the film was about 6.0 mg cm⁻² calculated by the difference between the weight of NiAl-LDH film on substrate and nickel foam substrate and ICP results (The element Ni resourced from the substrate has been considered). Through the EDS spectrum of NiAl-LDH film, we can see that the Ni/Al molar ratio was about 2.29 (Seen inset of Fig. 1b, other peaks occurred in the pattern were in correspondence with SEM gold spraying process). In addition, we used ICP to test that the Ni/Al molar ratio was about 2.26, in agreement with the EDS result. About 0.163 g MMO film was obtained after the process of thermal decomposition of LDHs at 400 °C to remove the interlayer anions. As shown in the SEM image (Fig. 1d), the layer of MMO remained the staggered nanosheet morphology of LDHs and open-pore structure. This is mainly because the response of dehydration, dehydroxylation and CO₃²⁻ delamination was carried out on the host layer of LDH sheets in the process of thermal decomposition of LDHs. We also found that the crystals of NiAl-LDH were not detached from the substrate after calcination. It shows that there is a strong binding force between MMO film and the 3D substrate.

Fig. 2 shows the XRD patterns of the NiAl-LDH and NiAl-MMO powders that scraped from the nickel foam substrates. The XRD pattern of the NiAl-LDH powder (Fig. 2a) displays some clear peaks that corresponded to (003), (006), (012) and (015) planes of the LDH crystals which exhibited the reflections characteristic of a NiAl-LDH (Joint Committee on Powder Diffraction Standards (JCPDS) file No. 15-0087). The calculated cell constants are $a = 3.01$ and $c = 23.40$ Å, in good agreement with the literature values.²⁷ The FT-IR spectrum of the powder scraped from NiAl-LDH films (Fig. 3a) is identical to that of the NiAl-LDH sediment (Fig. 3b), with a characteristic intense peak

due to the interlayer carbonate ion [v₃(CO₃)] at around 1353 cm⁻¹. However, it is known that dense NiAl carbonate LDH films were grown on the surface of nickel foam substrates. The 3D NiAl-MMO film was obtained by calcination of NiAl-LDH film precursor at temperature of 400 °C. Diffraction peaks (111), (200), (220) of Ni-like mixed oxide are observed in the XRD pattern (Fig. 2b).

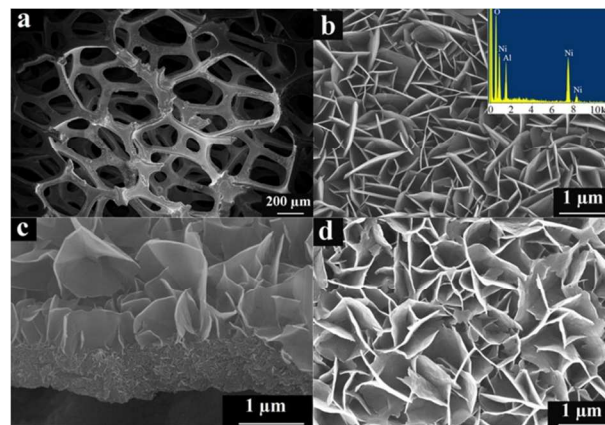


Fig. 1 SEM images of NiAl-LDH and NiAl-MMO films: (a) NiAl-LDH film on nickel foam, (b) enlarged surface of NiAl-LDH film on the surface (inset: an EDS spectrum of NiAl-LDH film), (c) edge of NiAl-LDH film on nickel substrate, and (d) surface of NiAl-MMO film (d).

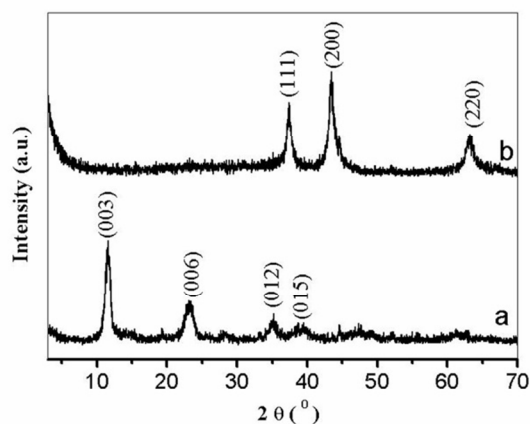


Fig. 2 XRD patterns of NiAl-LDH (a) and NiAl-MMO (b) powders scraped from the corresponding films.

Electrochemical and CDI Properties

The electrochemical performances of the 3D NiAl-MMO film as electrode material for electrosorption were tested using cyclic voltammograms (CVs) in 0.01 mol L⁻¹ NaCl aqueous solution in the potential range 0 – 0.6 V vs Ag/AgCl. Fig. 4a shows the CV curves of NiAl-MMO electrode at different scan rates. The shapes of the CV reveal that the capacitance characteristic was different from that of traditional electric double-layer capacitance in which the shape was normally an ideal rectangular shape. For each curve, the set of redox peaks observed indicate the existence of a Faradic process which was ascribed to the interconversion of Ni(II) ↔ Ni(III).²⁸ The position of the peaks which occurred as

a symmetrical shape appear at about 0.2 V in the CV curves measured at 5 mV s⁻¹ indicating a typical pseudocapacitive behavior arising from the reversible Faradaic transitions and the electroadsorption process is reversible. The result means that ions would be adsorbed on the electrode surface by forming an electric double layer and/or electrochemical reaction. Therefore, the specific capacitance (C) is indicating that the electroadsorption rate and capacity of NiAl-MMO electrode. C was calculated from galvanostatic discharge curves (Fig. 4b) using the following equation:

$$C = \frac{I \times \Delta t}{\Delta V \times m}$$

where I , Δt , ΔV , and m are the discharge current, the discharge time, the potential difference during the discharge (excluding the portion of the sudden potential drop), and the mass of NiAl-
MMO film, respectively. The result of specific capacitance resulted in a value of 114.2 F g⁻¹, 88.4 F g⁻¹, 62.6 F g⁻¹ and 47.9 F g⁻¹ at a charge and discharge current density of 5 mA cm⁻², 10 mA cm⁻², 20 mA cm⁻² and 30 mA cm⁻², respectively. A pure nickel foam (details are shown in Fig. S1 ESI†) and a NiAl-LDH film (Fig. S2 ESI†) were also tested as electrode materials using cyclic voltammograms and galvanostatic discharge curves. For nickel foam, although the redox peaks are symmetrical (Fig. S1a ESI†), but some of the galvanostatic discharge curves are incomplete because the discharge did not completely (Fig. S1b ESI†). The C of nickel foam was calculated to be only about 5.0 F g⁻¹ at 5 mA cm⁻², far less than that of NiAl-
MMO film. Therefore, the pure nickel foam can't be used as CDI electrode. For NiAl-LDH film, the redox peaks occurred as an asymmetrical shape (Fig. S2a ESI†), which means the electroadsorption process would be irreversible. And, the C of NiAl-LDH film was calculated to be ca. 77.4 F g⁻¹ at 5 mA cm⁻², also less than that of NiAl-
MMO film which should be attributed to the influence of interlayer carbonate ions. These results indicate that the well-
designed 3D NiAl-
MMO film should exhibit excellent electroadsorption performance.

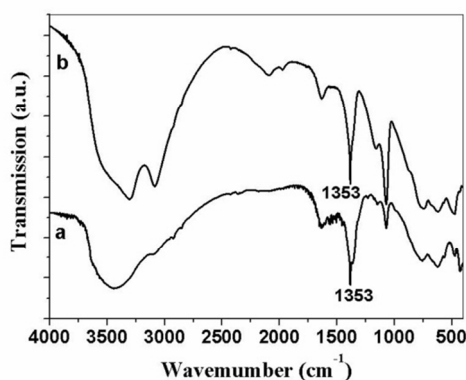


Fig. 3 FT-IR spectra of NiAl-LDH powder that scraped from the nickel foam substrate (a) and NiAl-LDH precipitation (b).

The 3D NiAl-
MMO film was used as electrode for the electroadsorption of NaCl in 0.01 mol L⁻¹ of NaCl solution. Fig. 5a

shows the desalination of an electroadsorption and desorption cycle of a NiAl-
MMO electrode by applying a direct voltage of 1.2 V. We can found from Fig. 5a that electroadsorption equilibrium time was about 60 min and the electroadsorption ratio was above 37.5%, while its desorption equilibrium time was about 30 min and desorption ratio was above 87.7%. According to the weight of NiAl-
MMO film electrode (about 0.163 g), the electroadsorptive capacity is an ultrahigh value of about 81.2 mg g⁻¹ NiAl-
MMO film electrode. Fig. 5b shows the curve of 15 electroadsorption and desorption cycles in 0.01 mol L⁻¹ NaCl solution. It is seen that the process of electroadsorption and desorption could be carried out easily in 90 min. However, the ions adsorbed in the first cycle could not be completely desorbed, but there was a very little change in electroadsorption and desorption ratio from second to fifteenth cycle. The CDI performances of NiAl-LDH film were also tested in 0.01 mol L⁻¹ of NaCl solution (Fig. S3 ESI†). The electroadsorption equilibrium time was about 30 min and the electroadsorption ratio was ca. 11.8%, while its desorption equilibrium time was about 25 min and desorption ratio was ca. 44.9%. Obviously, the CDI performances of NiAl-LDH film are much lower than that of NiAl-
MMO film and the interlayer carbonate ions of NiAl-LDH may be limit the chloride ions entering into the interlayer.

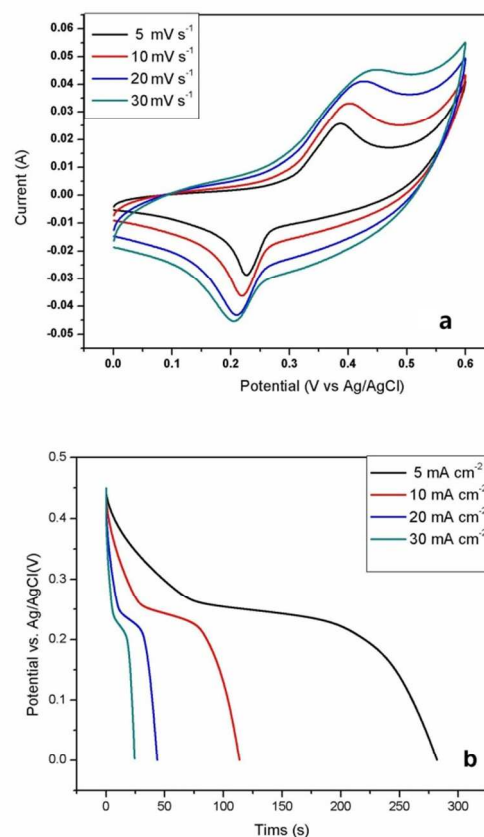


Fig. 4 Electrochemical characterizations of NiAl-
MMO film on nickel. (a) CV curves at different scan rates (5 – 30 mV s⁻¹); (b) galvanostatic discharge curves at various discharge current densities (5 – 30 mA cm⁻²).

According to reference 6(d) and our result, the Table 1 lists the electrosorption ratio, desorption ratio and electrosorption equilibrium time of some different electrodes and NiAl–MMO film electrode. Noting that the area of the electrodes in the literature 6(d) is 26 mm × 50 mm, which is more than two times of NiAl–MMO film electrode (20 mm × 30 mm). As is seen from Table 1, for NiAl–MMO film electrode, the electrosorption and desorption ratios are distinctly higher than those of activated carbon (AC) and AC fibre electrodes, just a little lower than that of AC–TiO₂ electrode. Although electrosorption ratio is a little

lower than that of CNT, but the desorption ratio is much higher than that of CNT. Moreover, all the electrosorption equilibrium times of AC, AC–TiO₂ and CNT electrodes are more than 200 min that were 3 times higher than that of our NiAl–MMO film electrode (60 min). Due to NiAl–MMO film electrode has the shortest electrosorption equilibrium time, higher electrosorption and desorption ratios, it has the best comprehensive properties and the electrode derived from NiAl–LDH film would be promising in the CDI industry.

Table 1. Electrosorption properties comparison of different electrodes.^{6d}

Kind of electrode	AC	AC–TiO ₂	AC fibre	CNT	Our NiAl–MMO
Size of electrode (mm×mm)	26×50	26×50	26×50	26×50	20×30
Initial concentration of NaCl solution (mg L ⁻¹)	500	500	500	500	585 (0.01 mol L ⁻¹)
Volume of NaCl solution (mL)	20	20	20	20	60
Direct voltage (V)	1.2	1.2	1.2	1.2	1.2
Reverse voltage (V)	-1.2	-1.2	-1.2	-1.2	-1.2
Electrosorption ratio (%)	27.5	44.9	13.8	51.6	37.5
Desorption ratio (%)	67.3	89.8	55.9	44.6	87.7
Electrosorption equilibrium time (min)	210	210	50	310	60

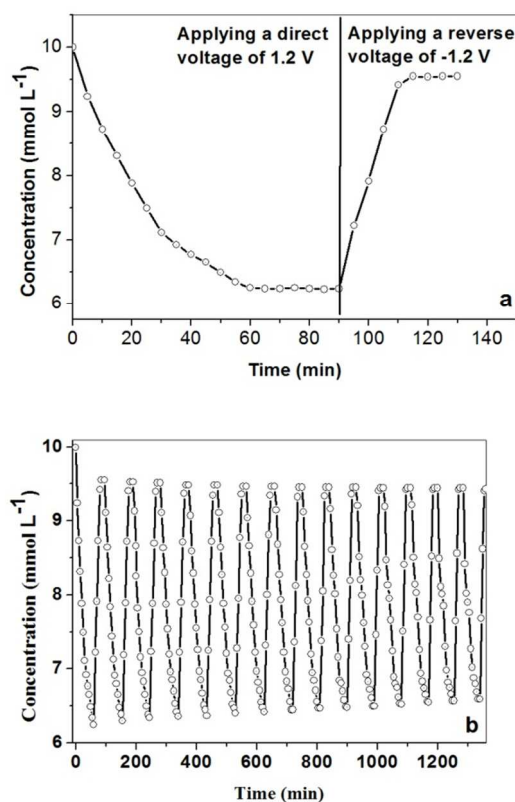


Fig. 5 Electrosorption and desorption equilibrium curve (a) and electrosorption and desorption cycles (b) of NiAl–MMO electrode in 0.01 mol L⁻¹ NaCl solution.

Regeneration of NiAl–MMO Film Electrodes

One of the advantages of electrosorption is the regeneration of electrode. When electrodes are saturated, ions can flee from the

electrodes by repulsive force by changing the polarity of electrodes, and then the electrodes are regenerated. Fig. 6a and b are the SEM images of 3D NiAl–MMO film after 15 electrosorption and desorption cycles in 0.01 mol L⁻¹ NaCl solution, which show that the MMOs on the film maintained sheet structure. Fig. 6c is the HRTEM image of an individual sheet for the NiAl–MMO film after 15 electrosorption and desorption cycles in NaCl solution. It reveals the presence of an interplanar distance of about 0.228 nm that is characteristic of the (111) plane, confirming the maintenance of NiAl–MMO phase. The interplanar distance is in agreement with the HRTEM image of an individual sheet for the NiAl–MMO film without used for electrosorption (about 0.230 nm, Fig. 6d). Fig. 7a is the XRD pattern of NiAl–MMO film after 15 electrosorption and desorption cycles in 0.01 mol L⁻¹ NaCl solution. It is the same as Fig. 2b that is the pattern of the NiAl–MMO film was obtained by calcination of NiAl–LDH film precursor at temperature of 400 °C for 3 h. The diffraction peaks (111), (200), (220) of NiAl–MMO are observed in both Fig. 7a and Fig. 2b. It is indicated that, after 15 electrosorption and desorption cycles, NiAl–MMO did not change into NiAl–LDH. However, LDH phase is observed when NiAl–MMO film was directly soaked in 0.01 mol L⁻¹ NaCl solution for 10 h, showing that the NiAl–MMO film recovered to LDH by structure “memory effect” (Fig. 7b). Therefore, these results confirm again that the electrosorption process is reversible, that is, Cl⁻ anions could be adsorbed on the NiAl–MMO film electrode surface by forming an electric double layer, and can flee from the electrodes by changing the polarity of electrodes, and the electrodes were regenerated. In addition, we found no Ni and Al ions appearing in the NaCl solution after electrosorption and desorption 15 cycles. It indicates that the NiAl–MMO film and nickel foam were not dissolved during the process and the electrosorption is physisorption. 3D nickel foam with high porosity and excellent physical strength was used as the substrate and the source of Ni²⁺ for the synthesis of 3D NiAl–MMO film electrode. The high porosity of nickel foam provided more channels to facilitate fast

penetration of the electrolyte. In other words, these channels ensure that enough Cl^- anions contracted with the surface of NiAl-MMO in a short time, ensuring the high use of the active material. The excellent electrosorption performances of NiAl-MMO film including high NaCl electrosorption and desorption ratios, fast electrosorption rate and good reversibility are directly related to the 3D porous and open pore structures.

Recently, a macroporous material composed of graphene nanosheets has been reported, which exhibited ultrahigh CDI performances with a superior electrosorptive capacity of about 4.95 mg g^{-1} and a fast desorption rate of 25 min.²⁹ Yin *et al.* also reported that 3D Graphene/ TiO_2 nanoparticle hybrid had the maximum electrosorptive capacity of about 25.0 mg g^{-1} , and could quickly reach electrosorption equilibrium (within 200 s), which is much shorter than AC (more than 800 s) and other reported materials.³⁰ The high electrosorption and desorption ratios and good reversibility of our 3D NiAl-MMO electrode with ultrahigh electrosorptive capacity of about 81.2 mg g^{-1} , is much higher than the best recorded for electrosorption electrodes.^{29,30} Taking advantage of its excellent electrosorption performances and low cost, the synthesized continuous dense NiAl-MMO film is promising alternative materials to nickel based oxide/hydroxide materials for use in noncarbon CDI electrode.

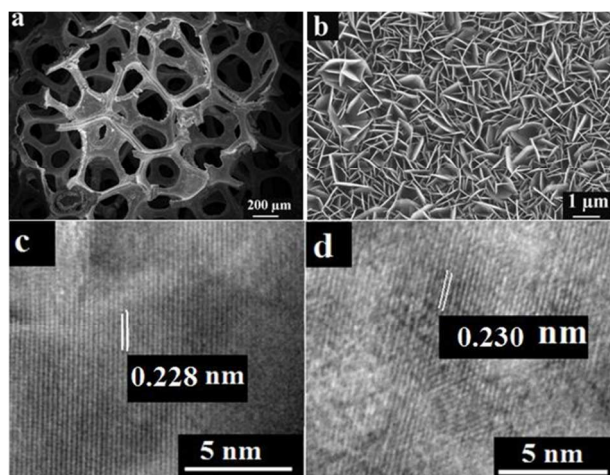


Fig. 6 The SEM (a, b) and of HRTEM (c) images of NiAl-MMO film after 15 electrosorption and desorption cycles in 0.01 mol L^{-1} NaCl solution, and HRTEM image of the NiAl-MMO film without treatment (d).

Conclusions

The NiAl-LDH film was grown on the surface of nickel foam by a simple in situ method. Then the 3D NiAl-MMO film, obtained after the NiAl-LDH film had been calcined for 3 h at $400 \text{ }^\circ\text{C}$, was employed as the electrode for an electrosorption application. In 0.01 mol L^{-1} NaCl solution, the electrosorption ratio is about 37.5%, while its desorption ratio is above 87.7% and electrosorptive capacity reached ultrahigh 81.2 mg g^{-1} electrode. The NiAl-MMO film electrode has good regeneration performance and there was a little change in electrosorption efficiency from the first cycle to the fifteenth cycle. The practicality comparison of AC, AC- TiO_2 , ACF, CNT, and

NiAl-MMO film electrode shows that NiAl-MMO film electrode is more suitable for the future industry applications of CDI with relatively higher electrosorption and desorption ratios as well as the shorter electrosorption equilibrium time. Further study of the CDI properties of NiAl-MMO film for the higher concentration NaCl solutions, potential applications in some other salt aqueous solutions and scaling up for practical CDI industrial application is underway in our laboratory.

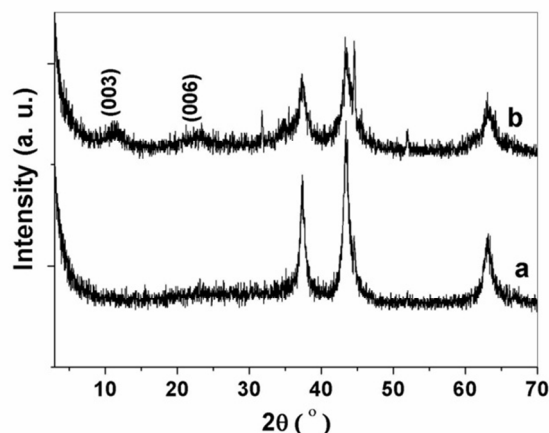


Fig. 7 The XRD patterns of NiAl-MMO film after 15 electrosorption and desorption cycles in 0.01 mol L^{-1} NaCl solution (a) and NiAl-MMO film after soaked in NaCl solution for 10 h (b).

Acknowledgements

This research project financially supported by the 973 Program (No. 2014CB932104), 863 Program (No. 2012AA03A609), NSFC and the Program for Changjiang Scholars and Innovative Research Team in University (no. IRT1205) of P. R. China.

Notes and references

State Key Laboratory of Chemical Resource Engineering, Beijing University of Chemical Technology, PO Box 98, Beijing 100029, China. Tel.: +86-10-64453537; Fax: +86-10-64425385; E-mail address: leixd@mail.buct.edu.cn (X. Lei).

- † Electronic Supplementary Information (ESI) available: CV curves at different scan rates ($5 - 30 \text{ mV s}^{-1}$) and galvanostatic discharge curves at various discharge current densities ($5 - 30 \text{ mA cm}^{-2}$) of nickel foam and NiAl-LDH film, respectively; Electrosorption and desorption equilibrium curve of NiAl-LDH electrode in 0.01 mol L^{-1} NaCl solution. See DOI: 10.1039/b000000x/
- (a) M. A. Shannon, P. W. Bohn, M. Elimelech, J. G. Georgiadis, B. J. Mariñas and A. M. Mayes, *Nature*, 2008, **452**, 301; (b) R. P. Schwarzenbach, B. I. Escher, K. Fenner, T. B. Hofstetter, C. A. Johnson, U. Von Gunten and B. Wehrli, *Science*, 2006, **313**, 1072.
 - (a) H. Li, L. Pan, Y. Zhang, L. Zou, C. Sun, Y. Zhan and Z. Sun, *Chem. Phys. Lett.*, 2010, **485**, 161; (b) L. Zou, L. Li, H. Song and G. Morris, *Water Res.*, 2008, **42**, 2340.
 - (a) C.-M. Yang, W.-H. Choi, B.-K. Na, B. W. Cho and W. I. Cho, *Desalination*, 2005, **174**, 125; (b) Y.-J. Kim and J.-H. Choi, *Sep. Purif. Technol.*, 2010, **71**, 70.
 - Y. Han, X. Quan, X. Ruan and W. Zhang, *Sep. Purif. Technol.*, 2008, **59**, 43.
 - L. Zou, G. Morris and D. Qi, *Desalination*, 2008, **225**, 329.
 - (a) L. Li, L. Zou, H. Song and G. Morris, *Carbon*, 2009, **47**, 775; (b) K.-K. Park, J.-B. Lee, P.-Y. Park, S.-W. Yoon, J.-S. Moon, H.-M. Eum and C.-W. Lee, *Desalination*, 2007, **206**, 86; (c) Y. Gao, L.

- Pan, H. Li, Y. Zhang, Z. Zhang, Y. Chen and Z. Sun, *Thin Solid Films*, 2009, **517**, 1616; (d) L. M. Chang, X. Y. Duan and W. Liu, *Desalination*, 2011, **270**, 285.
- 7 A. Afkhami and B. E. Conway, *J. Colloid Interface Sci.*, 2002, **251**,
5 248.
- 8 (a) D. G. Evans and X. Duan, *Chem. Commun.*, 2006, 485; (b) G. R.
Williams and D. O'Hare, *J. Mater. Chem.*, 2006, **16**, 3065.
- 9 X. Yu, Z. Chang, X. Sun, X. Lei, D. G. Evans, S. Xu and F. Zhang,
Chem. Eng. J., 2011, **169**, 151.
- 10 (a) X. Qiu, K. Sasaki, T. Hirajima, K. Ideta and J. Miyawaki, *Chem.*
Eng. J., 2013, **225**, 664; (b) Q. Guo, Y. Zhang, Y. Cao, Y. Wang
and W. Yan, *Environ. Sci. Pollut. Res.*, 2013, **20**, 8210; (c) L. Xiao,
W. Ma, M. Han and Z. Cheng, *J. Hazard. Mater.*, 2011, **186**, 690.
- 11 D. Shan, S. Cosnier and C. Mousty, *Anal. Chem.*, 2003, **75**, 3872.
- 12 Z. Lu, W. Zhu, X. Lei, G. R. Williams, D. O'Hare, Z. Chang, X. Sun
and X. Duan, *Nanoscale*, 2012, **4**, 3640.
- 13 (a) F. Zhang, L. Zhao, H. Chen, S. Xu, D. G. Evans and X. Duan,
Angew. Chem. Int. Ed., 2008, **47**, 2466; (b) F. Zhang, M. Sun, S. Xu,
L. Zhao and B. Zhang, *Chem. Eng. J.*, 2008, **141**, 362.
- 14 R. Liang, S. Xu, D. Yan, W. Shi, R. Tian, H. Yan, M. Wei, D. G
Evans and X. Duan, *Adv. Funct. Mater.*, 2012, **22**, 4940.
- 15 (a) J. Qiu and G. Villemure, *J. Electroanal. Chem.*, 1995, **395**, 159;
(b) R. Roto, A. Yamagishi and G. Villemure, *J. Electroanal. Chem.*,
2004, **572**, 101.
- 16 J. Wang, Y. Song, Z. Li, Q. Liu, J. Zhou, X. Jing, M. Zhang and Z.
Jiang, *Energy Fuels*, 2010, **24**, 6463.
- 17 (a) H. Chen, F. Zhang, S. Fu and X. Duan, *Adv. Mater.*, 2006, **18**,
3089; (b) Z. Lü, F. Zhang, X. Lei, L. Yang, S. Xu and X. Duan,
Chem. Eng. Sci., 2008, **63**, 4055; (c) X. Lei, L. Wang, X. Zhao, Z.
Chang, M. Jiang, D. Yan and X. Sun, *Ind. Eng. Chem. Res.*, 2013,
30 **52**, 17934; (d) Y. Gu, Z. Lu, Z. Chang, J. Liu, X. Lei, Y. Li and X.
Sun, *J. Mater. Chem. A*, 2013, **1**, 10655.
- 18 G.-W. Yang, C.-L. Xu and H.-L. Li, *Chem. Commun.*, 2008, 6537.
- 19 R. R. Salunkhe, B. P. Bastakoti, C.-T. Hsu, N. Suzuki, J. H. Kim, S.
X. Dou, C.-C. Hu and Y. Yamauchi, *Chem. Eur. J.*, 2014, **20**, 3084.
- 20 U. M. Patil, J. S. Sohn, S. B. Kulkarni, S. C. Lee, H. G. Park, K. V.
Gurav, J. H. Kim and S. C. Jun, *ACS Appl. Mater. Interfaces*, 2014,
6, 2450.
- 21 G. Wang, D. Cao, C. Yin, Y. Gao, J. Yin and L. Cheng, *Chem.*
40 *Mater.*, 2009, **21**, 5112.
- 22 B. Liu, B. Liu, Q. Wang, X. Wang, Q. Xiang, D. Chen and G. Shen,
ACS Appl. Mater. Interfaces, 2013, **5**, 10011.
- 23 Y. Yu, C.-H. Chen, J.-L. Shui and S. Xie, *Angew. Chem. Int. Ed.*,
2005, **44**, 7085.
- 24 L. Zhang, C. Tang, X. Yin and H. Gong, *J. Mater. Chem. A*, 2014, **2**,
45 4660.
- 25 S. Cai, D. Zhang, L. Shi, J. Xu, L. Zhang, L. Huang, H. Li and J.
Zhang, *Nanoscale*, 2014, **6**, 7346.
- 26 H. Zhang, X. Yu and P. V. Braun, *Nature Nanotechnol.*, 2011, **6**, 277.
- 27 (a) S. Velu, K. Suzuki, M. Kapoor, S. Tomura, F. Ohashi and T.
50 Osaki, *Chem. Mater.*, 2000, **12**, 719; (b) V. Prevot, N. Caperaa, C.
Taviot-Gueho and C. Forano, *Cryst. Growth Des.*, 2009, **9**, 3646.
- 28 Z. Lu, Z. Chang, W. Zhu and X. Sun, *Chem. Commun.*, 2011, 9651.
- 29 Z. Y. Yang, L. J. Jin, G. Q. Lu, Q. Q. Xiao, Y. X. Zhang, L. Jing, X.
55 X. Zhang, Y. M. Yan and K. N. Sun, *Adv. Funct. Mater.*, 2014, **24**,
3917.
- 30 H. Yin, S. Zhao, J. Wan, H. Tang, L. Chang, L. He, H. Zhao, Y. Gao
and Z. Tang, *Adv. Mater.*, 2013, **25**, 6270.